Substrate Translocation Kinetics of Excitatory Amino Acid Carrier 1 Probed with Laser-Pulse Photolysis of a New Photolabile Precursor of D-Aspartic Acid[†]

Christof Grewer,*[,‡] Sayed Abdollah Madani Mobarekeh,[§] Natalie Watzke,[‡] Thomas Rauen,[⊥] and Klaus Schaper[§]

Max-Planck-Institut für Biophysik, Kennedyallee 70, D-60596 Frankfurt, Germany, Institut für Organische Chemie und Makromolekulare Chemie I, Heinrich-Heine-Universität Düsseldorf, Universitätstrasse 1, D-40225 Düsseldorf, Germany, and Max-Planck-Institut für Hirnforschung, Deutschordenstrasse 46, D-60528 Frankfurt, Germany

Received July 10, 2000; Revised Manuscript Received October 12, 2000

ABSTRACT: Here we report the synthesis and photochemical and biological characterization of a new photolabile precursor of D-aspartic acid, α-carboxynitrobenzyl-caged D-aspartate (α-CNB-caged D-aspartate), and its application for studying the molecular mechanism of the neuronal excitatory amino acid carrier 1 (EAAC1). Investigation of the photochemical properties of α-CNB-caged D-aspartate by transient absorption spectroscopy of the *aci*-nitro intermediate revealed that it photolyzes with a quantum yield of 0.19 at pH 7.0. The major component of the *aci*-nitro intermediate (77% of the total absorbance) decays with a time constant of 26 μs. This decay is slowed by only a factor of 2 when increasing the pH to 10. A minor component (21%) decays with a time constant of 410 μs and is pH insensitive. The compound was tested with respect to its biological activity with the glutamate transporter EAAC1 expressed in HEK293 cells. Whole-cell current recordings from these cells in the presence and absence of α-CNB-caged D-aspartate demonstrated that the compound neither activates nor inhibits EAAC1. Upon photolysis, D-aspartate-mediated whole-cell currents were generated. In contrast to laser-pulse photolysis experiments with α-CNB-caged L-glutamate, only a minor and much slower transient current component was observed. These results indicate that the substrate translocation step, which is not rate-limiting for the overall turnover of the transporter with L-glutamate, becomes rate-limiting when D-aspartate is translocated. The results demonstrate that the new caged D-aspartate derivative is a useful tool for the investigation of the molecular mechanism of glutamate transporters and probably other aspartate translocating systems using rapid chemical kinetic techniques.

Glutamate is the major excitatory neurotransmitter in the mammalian brain (*1*). It mediates synaptic signal transmission by binding to and activating postsynaptic ionotropic and metabotropic glutamate receptors. After completion of the signal transmission process, glutamate is removed from the synapse by (i) passive diffusion (*2*) and (ii) active transport into neurons and adjacent glial cells (*3*). This reuptake of glutamate is accomplished by high affinity plasma membrane transporters and is driven by the concentration gradients for sodium and potassium across the membrane (*4*−*6*). To obtain a better understanding of the glutamate transport process, it is important to study the molecular reactions of glutamate transporters by time-resolved techniques with an optimal time resolution of microseconds to milliseconds.

Recently, we have used a rapid chemical kinetic technique that is based on the photolysis of caged glutamate to investigate the individual reaction steps of the glutamate transporter EAAC1 (excitatory amino acid carrier 1)[1] in detail (*21*). Laser-induced photolysis of a photolabile, inactive precursor of glutamate (caged glutamate) within less than 100 μs was applied to produce rapid glutamate concentration jumps for the activation of glutamate transporters. This method overcomes problems with slow mixing or diffusion of reactants. One of the results of this study was that Na^+-driven glutamate translocation of EAAC1 occurs on a millisecond time scale and is, therefore, not rate-limiting for the steady-state turnover of the transporter that takes place with a time constant in the range of 35 ms. The turnover rate, however, depends on the type of the transported substrate. D-Glutamate, L-aspartate, and D-aspartate are recognized by the transporter as substrates but are transported at a slower steady-state rate than L-glutamate (*7*). Therefore, it appears likely that there is a shift in the rate-limiting step of the transporter when these substrates are used instead of L-glutamate. The availability of one of these compounds in caged form would provide a tool for the investigation of these important issues.

Various different photolabile protecting groups were developed in the past (*8*). One of these groups, the α-car-

[†] Supported by the Deutsche Forschungsgemeinschaft (Grant GR 1393/2-1 to C.G.).

* To whom correspondence should be addressed. Christof Grewer, Ph.D., Max-Planck-Institut für Biophysik, Kennedyallee 70, D-60596 Frankfurt, Germany, Tel: +49-69-6303-336, Fax: +49-69-6303-305, E-mail: grewer@mpibp-frankfurt.mpg.de.

[‡] Max-Planck-Institut für Biophysik.

[§] Heinrich-Heine-Universität Düsseldorf.

[⊥] Max-Planck-Institut für Hirnforschung.

[1] Abbreviations: EAAC1: excitatory amino acid carrier 1; EAAT3: excitatory amino acid transporter 3; GLAST: glutamate aspartate transporter; α-CNB: α-carboxy-2-nitrobenzyl; HEK: human embryonic kidney; NBS: *N*-bromosuccinimide; DBU: 1,8-diazabicyclo-[5.4.0]undec-7-ene; TFA: trifluoroacetic acid; GABA: γ-aminobutyric acid; NMDA: *N*-methyl-D-aspartic acid.

10.1021/bi0015919 CCC: $20.00
Published on Web 12/09/2000

Scheme 1

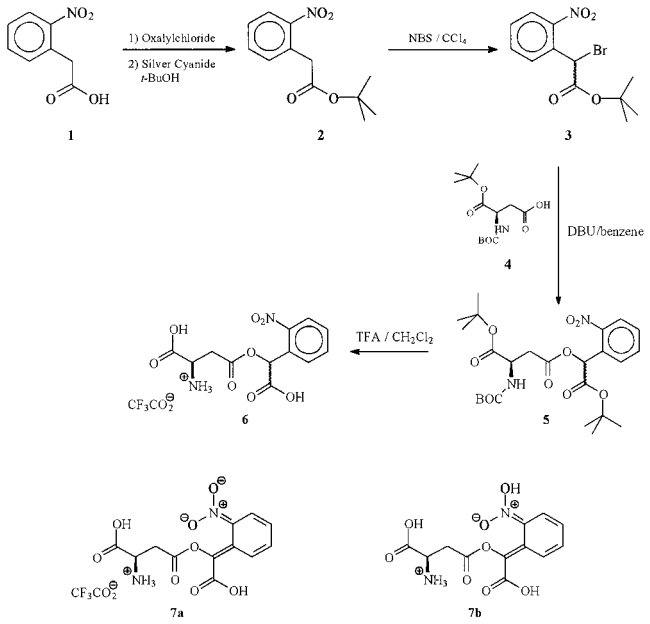

boxy-2-nitrobenzyl (α-CNB) moiety, has proven very effective for protecting carboxylic acids, such as a variety of different neurotransmitters (*9*−*14*). These caged compounds were used in many studies of rapid kinetics of neurotransmitter receptors and, in addition, for locating functional receptors on cell surfaces and circuits of nerve cells (*15*−*17*).

Here, we describe the synthesis (Scheme 1) and photochemical properties of a new caged derivative of D-aspartic acid. As coupling reagent an α-brominated *t*-butyl ester of the α-CNB moiety was synthesized by an improved method analogous to a procedure described by Takimoto (*18*). This bromide was attached to an α- and N-diprotected D-aspartic acid and after hydrolysis of the ester and amide protecting groups the desired product was obtained. The compound exhibits favorable photochemical and biological properties and is demonstrated to be useful for rapid kinetic investigations of the glutamate transporter subtype EAAC1. The results show that in contrast to glutamate transport the aspartate translocation step becomes rate-limiting in the transport cycle of EAAC1.

MATERIALS AND METHODS

General Remarks. For column chromatography, either silica gel 60 from Merck or Sephadex LH20 from Pharmacia was used. 300 MHz ^{1}H NMR were measured on a Varian VXR 300, and 500 MHz ^{1}H NMR were measured on a Bruker AM-500. Melting points were determined using a Reichardt Thermovar, Büchi 510.

tert-Butyl α-(2-nitrophenyl)acetate (**2**). Silver cyanide was prepared by mixing a solution of 2.0 g (31 mmol) sodium cyanide in 50 mL of water with a solution of 4.5 g (34 mmol) silver nitrate in 50 mL of water at room temperature. The precipitate was filtered off, washed with water, and dried at 0.1 mbar for 10 h. A suspension of 5.0 g (28 mmol) α-(2-nitrophenyl)acetic acid (**1**) and 5.2 g (41 mmol) oxalyl chloride in 50 mL of absolute benzene was stirred for 20 h at room temperature under nitrogen. The remaining oxalyl chloride was evaporated under reduced pressure at room temperature. The acid chloride was obtained as clear yellow liquid, which was added to a stirred mixture of 8.0 g (60 mmol) of freshly prepared silver cyanide (see above) and 3.0 g (41 mmol) of *tert*-butyl alcohol in 20 mL of absolute benzene. The mixture was heated to reflux for 8 h and allowed to cool to room temperature. Then this mixture was filtered through a silica gel column, washed with a saturated solution of sodium bicarbonate (3 × 20 mL) and water, dried over sodium sulfate, and concentrated to give 6.0 g (25 mmol, 91%) of compound **2** as a yellow oil. ^{1}H NMR ($CDCl_3$, 500 MHz) 8.08 (dd, $^3J_{HH}$ = 8.17 Hz, $^4J_{HH}$ = 1.32 Hz, 1H, Ar-3-H), 7.57 (dt, $^3J_{HH}$ = 7.53 Hz, $^4J_{HH}$ = 1.34 Hz, 1H, Ar-5-H), 7.45 (dt, $^3J_{HH}$ = 7.81 Hz, $^4J_{HH}$ = 1.48 Hz, 1H, Ar-4-H), 7.33 (dd, $^3J_{HH}$ = 7.61 Hz, $^4J_{HH}$ = 1.26 Hz, 1H, Ar-6-H), 3.93 (s, 2H, $ArCH_2$), 1.43 (s, 9H, $C(CH_3)_3$).

tert-Butyl α-bromo-α-(2-nitrophenyl)acetate (**3**). A mixture of 3.0 g (13 mmol) of ester **2**, 2.5 g (14 mmol) of *N*-bromosuccinimide (NBS), and catalytic amounts of dibenzoyl peroxide in 25 mL of tetrachloromethane was heated to reflux for 72 h. The mixture was allowed to cool to room temperature, the succinimide and unreacted NBS was filtered off, and the filtrate was charged with 1.50 g (8.43 mmol) of NBS and catalytic amounts of dibenzoyl peroxide and heated under reflux for a further 48 h. The precipitate was filtered off again, and the filtrate was concentrated under reduced pressure to a pale yellow oil. The product was separated from the starting material via column chromatography (silica gel, *n*-hexane/ethyl acetate 3/1) to yield 2.4 g (7.6 mmol, 59%) of **3** as a yellow oil. ^{1}H NMR ($CDCl_3$, 500 MHz) 7.95 (dd, $^3J_{HH}$ = 8.10, $^4J_{HH}$ = 1.36 Hz, 2H, Ar-3-H, Ar-6-H), 7.65 (dt, $^3J_{HH}$ = 7.68, $^4J_{HH}$ = 1.33 Hz, 1H, Ar-5-H), 7.48 (dt, $^3J_{HH}$ = 7.79, $^4J_{HH}$ = 1.40 Hz, 1H, Ar-4-H), 5.93 (s, 1H, ArCH), 1.44 (s, 9H, $C(CH_3)_3$).

N-(t-Butoxycarbonyl)-4-O-[α-(tert-butoxycarbonyl)-2-nitrobenzyl]-1-O-tert-butyl-R-aspartic acid (**5**). A mixture of 0.24 g (0.83 mmol) of *N*-(*t*-butoxycarbonyl)-1-*O*-*tert*-butyl-*R*-aspartic acid (**4**), 0.36 g (1.1 mmol) of *tert*-butyl α-bromo-α-(2-nitrophenyl)acetate **3**, and 0.24 g (1.6 mmol) of 1,8-diazabicyclo[5.4.0]undec-7-ene (DBU) in 30 mL of absolute benzene was heated under reflux for 5 h. The mixture was allowed to cool to room temperature and 20 mL of water was added to dissolve the solids. Twenty milliters of ethyl acetate was added, the organic phase was removed, and the aqueous phase was washed two times with ethyl acetate (20 mL). The combined organic layers were dried over sodium sulfate and concentrated under reduced pressure to yield a pale brown oil. The product was purified through column chromatography (silicagel, *n*-hexane/ethyl acetate 3/1). A total of 0.37 g (0.71 mmol, 85%) 1:1 mixture of diastereomers (estimated from the ^{1}H NMR integrals of the benzylic proton) of **5** was obtained as yellow oil. ^{1}H NMR ($CDCl_3$, 300 MHz) 8.03 (dd, $^3J_{HH}$ = 8.0 Hz, $^4J_{HH}$ = 1.1 Hz, 1H, Ar-3-H), 7.7−7.5 (m, 3H, Ar-4-H, Ar-5-H, Ar-6-H), 6.81, 6.78 (2 s, 1H, ArCH), 5.64, 5.56 (2 d, $^3J_{HH}$ = 8.2 Hz, $^3J_{HH}$ = 8.5 Hz, 1H, NH), 4.53−4.47 (m, 1H, NH−C*H*), 3.3−2.9 (m, 2H, CH_2), 1.45, 1.44, 1.43, 1.41, 1.40 (5 s, 27H, $C(CH_3)_3$). Anal. Calc. for $C_{25}H_{36}N_2O_{10}$: C, 57.24; H, 6.92; N, 5.34; Found: C, 57.43; H, 6.96; N, 5.08.

4-O-(α-Carboxy-2-nitrobenzyl)-R-aspartic acid hydro-trifluoroacetate (**6**). A solution of 0.24 g (0.45 mmol) of ester **5** in a mixture of 11 mL of dichloromethane and 4 mL of trifluoroacetic acid (TFA) was stirred at room temperature

under nitrogen for 16 h. The mixture was concentrated under reduced pressure, 20 mL toluene was added, and the solvent was evaporated again. This procedure was repeated once, and the residual brown oil was purified on Sephadex with water. After lyophylization of the sample, 0.13 g (0.30 mmol, 65%) of caged aspartic acid **6** was obtained as 1:1 mixture of diastereomers (estimated from the ^{1}H NMR integrals of the benzylic proton) as white solid. ^{1}H NMR (D_2O, 300 MHz) 8.2−8.0 (m, 1H, Ar-3-H), 7.9−7.7 (m, 1H, Ar-5-H), 7.7−7.6 (m, 2H, Ar-4-H, Ar-6-H), 6.69, 6.67 (2 s, 1H, Ar−CH), 4.6−4.5 (m, 1H, NH−C*H*), 3.3−3.1 (m, 2H, CH_2), mp: 112−114 °C.

Transient Absorption Measurements. Transient absorption spectroscopy was performed as described in detail previously (*9*, *13*). Briefly, pulsed laser light of 308-nm wavelength and 10-ns pulse duration (Lambda Physics EMG200, ≈50 mJ energy/pulse) was used to excite the caged compound in a quartz cuvette (2 × 10 mm path length, Hellma QS). The absorption change after laser excitation was measured with the light of a Xenon lamp (Zeiss, XBO 75W) passing through the 2-mm window of the sample cuvette perpendicular to the laser beam. The wavelength of the analysis light was selected with a monochromator (The Optometrics Group) in front of and behind the sample cuvette, and the light intensity as a function of time was measured with a PIN photodiode (Siemens). The signal of the photodiode was preamplified (Advanced Research Instruments, PMT-4), recorded with a digital oscilloscope (LeCroy, 9310AM), and stored on a floppy disk. The data were evaluated using MicroCal Origin v5.0.

Quantum Yield. The quantum yield was determined as described by measuring the absorbance (A_n) of the *aci*-nitro intermediate as a function of the number of consecutive laser-pulses (n) assuming that (i) the absorbance, and therefore the concentration of the *aci*-nitro intermediate, is directly proportional to the concentration of the liberated D-aspartic acid, and (ii) the absorbance of the solution is not a function of n because the irradiation wavelength is near the isosbestic point of starting material and photoproduct (*9*, *14*). The quantum yield ϕ can be calculated by the following equation from the slope of a plot of $\ln(A_n)$ versus $(n - 1)$:

$$\ln(A_n) = \ln\left(\epsilon_M l \phi \frac{n_A}{VF}\right) - \phi \frac{n_A}{c_0 V}(n-1) \qquad (1)$$

Here, l represents the path length of the analysis light, c_0 is the initial concentration of the caged compound, n_A is the number of absorbed photons, V is the total volume of the solution, and F is the fraction of the solution irradiated. The molar extinction coefficient of the *aci*-nitro intermediate, ϵ_M, can be estimated from the intercept.

Cell Culture and Transfection. Human embryonic kidney cells (HEK293, ATCC No. CRL 1573) were cultured as described previously (*19*). Transient transfection with the EAAC1 encoding construct pCMV-EAAC1 (40 μg/5 × 10^6 cells) was performed using the calcium phosphate coprecipitation method 1 day after subculture. At 1 day post-transfection, cells were used for electrophysiology.

Whole-Cell Current Recording. Glutamate transporter-associated currents were measured at room temperature in the whole-cell current-recording configuration (*20*) as described earlier (*21*). The intracellular solution contained 130 mM KSCN, 1 mM $MgCl_2$, 10 mM TEACl, 10 mM EGTA, and 10 mM HEPES (pH 7.3). The bath buffer solution contained 140 mM NaCl, 2 mM $MgCl_2$, 2 mM $CaCl_2$, and 10−30 mM HEPES (pH 7.3). The typical resistance of the recording electrode was 2−3 MΩ; the series resistance was 4−6 MΩ. Because of the small whole-cell currents (less than 200 pA) series resistance compensation was not necessary. The currents were amplified with an Adams & List EPC-7 amplifier, low pass filtered at 1−10 kHz (Krohn-Hite 3322), and digitized with a digitizer board (Axon, Digidata 1200) at a sampling rate of 10−50 kHz that was controlled by software (Axon PClamp).

Laser-Pulse Photolysis and Rapid Solution Exchange. Laser-pulse photolysis experiments were performed as described previously (*14*, *22*). Briefly, the cells were equilibrated with L-glutamate, D-aspartate, caged D-aspartate, or caged L-glutamate (Molecular Probes) using a fast solution exchange device (*23*). All compounds were dissolved in extracellular solution. Caged D-aspartate solutions were prepared freshly by dissolving the solid compound directly before each experiment. For short periods of time (1−6 h) the caged D-aspartate solutions could be stored at −20 °C in the dark without detectable increase in the background of free aspartate. The velocity of the solution emerging from the porthole of the device was 5 cm/s, and the time resolution was 20−30 ms (10−90% rise time with whole cells). The caged compounds were photolyzed with a light flash generated by an excimer laser (Lambda Physik, MINEX) pumped homemade dye laser using *p*-terphenyl as the laser dye (5 mM solution in dioxan, λ_{em} = 340 nm, $t_{1/2}$ = 15 ns). The laser light was delivered to the cell with an optical fiber (350 μm diameter). The laser energy was adjusted with neutral density filters (Andover Corporation). Typical laser energies were in the range of 50−400 mJ/cm^2. A standard D-aspartate concentration of 100 μM was applied to the cell by rapid solution exchange before and after laser-pulse photolysis to estimate the concentration of photolytically released D-aspartate and to test the cell for damage by the laser pulse (*22*).

RESULTS

The α-CNB caging group has been exploited for caging a number of biologically important carboxylates in the past (*10*−*12*, *14*). It was shown for the acidic amino acid glutamate that linkage to the γ-carboxy group is advantageous as compared to the α-ester with respect to stability in aqueous solution (*11*). Furthermore, the γ-(α-CNB-caged) L-glutamate exhibited favorable biological properties when used with ionotropic glutamate receptors (*11*). For these reasons, we chose to use the same strategy for the synthesis of a caged D-aspartate.

Kinetics and Quantum Yield of Photolysis. Irradiation of an aqueous solution of β-(α-CNB-caged) D-aspartate (100 μM) at 308 nm leads to photolysis of the compound as indicated by a distinct change of the UV−visible spectrum of the solution. The spectrum obtained after complete photolysis of the compound shows an increase of the absorbance at wavelengths higher than about 300 nm, which is typical for photoproducts associated with 2-nitrobenzyl photochemistry (*9*, *24*). In addition to the stationary absor-

bance change, pulsed irradiation of a α-CNB-caged D-aspartate containing solution at 308 nm produces a transient absorbance change on a microsecond time scale. The spectral distribution of this absorbance change which is red-shifted with respect to the ground-state spectrum is shown in Figure 1, panel A (inset), at several times after the laser flash. The spectrum displays a peak at a wavelength of 425 nm, indicative of an *aci*-nitro intermediate that is produced upon photolysis of 2-nitrobenzyl-caged compounds (*25*, *26*). To determine the rate constant of photocleavage, we measured the time dependence of the transient absorbance change after pulsed irradiation at 308 nm at a wavelength of 430 nm, close to the peak of the *aci*-nitro intermediate spectrum. It is commonly accepted for caged compounds based on the 2-nitrobenzyl group that the decay of the *aci*-nitro intermediate is rate-limiting for the overall reaction and can, therefore, be used to monitor the kinetics of photoproduct release (*27*, *28*). In line with results obtained for α-CNB-caged L-glutamate (*11*) the decay of the *aci*-nitro intermediate absorbance is biphasic (Figure 1, panel A). The fast component decays with a time constant of 26 ± 3 μs and contributes 77 ± 5% to the total absorbance ($n = 10$). The slow, minor component decays with a time constant of 410 ± 60 μs and its relative contributions to the total absorbance is 21 ± 5%. A stationary component of the absorbance that is caused by formation of the nitroso ketone byproduct has a relative amplitude of about 2%. These rate constants are in the same range as those determined for other, similar α-CNB-caged carboxylates. The biexponential decay of the transient absorbance change was detected in the past for a number of caged compounds based on the nitrobenzyl group (*11*−*14*). The spectral distribution is not considerably different between the two exponential components, suggesting that they both reflect the decay of a short-lived, conjugated intermediate, such as the *aci*-nitro compound.

The quantum yield of the photoreaction was determined by irradiating a 500 μM solution of caged D-aspartate with consecutive laser flashes of 308 nm. Product formation was monitored by measuring the absorbance of the *aci*-nitro intermediate. The logarithm of the maximum absorbance A was then plotted versus $(n - 1)$, and the quantum yield was obtained from the slope as 0.19 ± 0.01, similar to the quantum yield for α-CNB-caged L-glutamate (0.14), which was determined with a different method (*11*). From the intercept, the molar extinction coefficient of the *aci*-nitro intermediate was estimated as 3800 M^{-1} cm^{-1} at 430 nm and pH 7.0.

pH Dependence of the Photolysis Reaction. So far, we have characterized the photochemistry of α-CNB-caged D-aspartate in the physiological pH range. However, the glutamate transport process of EAAC1 is highly pH dependent (*29*, *30*). Therefore, we investigated the pH dependence of the photolysis reaction in greater detail to test whether the new caged derivative can be used at a pH much different from 7.0. The decay of the *aci*-nitro intermediate absorption is biphasic in the whole pH range studied. The decay rate constants of the fast and the slow phase as a function of pH are shown in Figure 1, panel B. Whereas the rate constant for the slowly decaying phase is almost pH independent, the rapidly decaying phase is moderately accelerated with increasing pH (about 1.3-fold/pH unit), consistent with the pH-dependent behavior observed for other α-CNB-caged

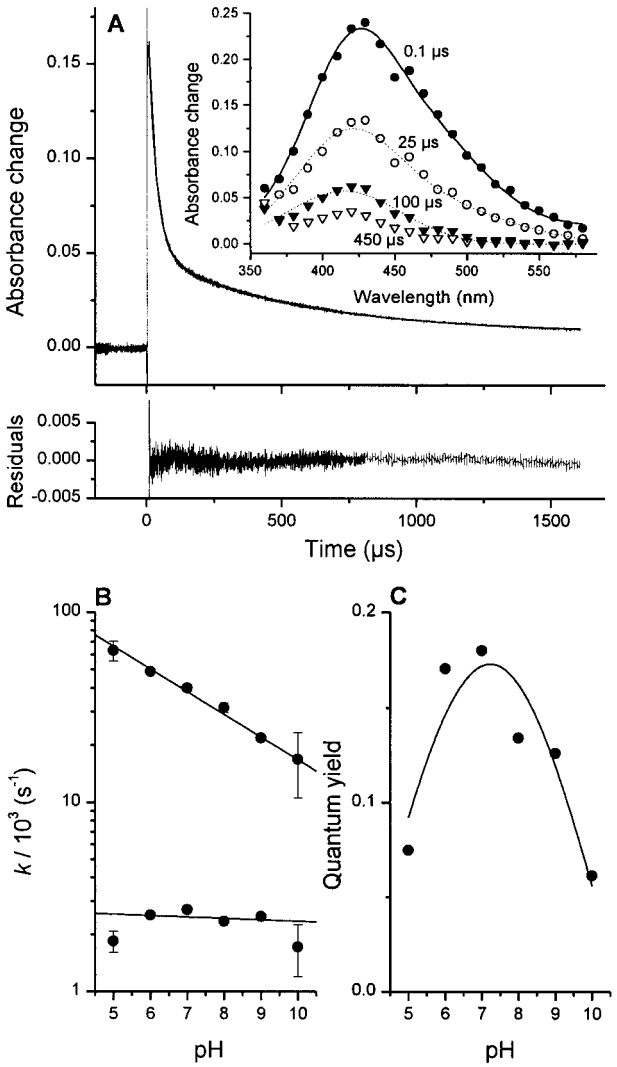

FIGURE 1: (A) Transient absorbance change produced by 1 mM α-CNB-caged D-aspartate after photolysis with a 10-ns, 308-nm laser flash. The wavelength of the analysis light was 430 nm with a path length of 10 mm. The solid line represents the best fit to a double exponential decay function. The time constants of the fast and the slow exponentials are 29 ± 1 μs and 530 ± 10 μs; their relative contributions to the total absorbance are 0.75 ± 0.05 and 0.21 ± 0.06, respectively. A nondecaying stationary component of the absorbance has a relative amplitude of 0.04 ± 0.01. The lower panel shows the fitting residuals. The conditions of the experiment were $T = 22$ °C and pH 7.0 (100 mM phosphate buffer). Inset: UV−visible spectrum of the transient absorbance change induced by 308 nm pulsed photolysis of 1 mM α-CNB-caged D-aspartate as a function of time ($T = 22$ °C and pH 7.0; 100 mM phosphate buffer). The spectra were recorded at times of (from top to bottom) 0.1, 25, 100, and 450 μs after the laser flash. (B) Rate constants of the decay of the fast (closed circles) and slow (open circles) exponential phases of the transient absorbance change as a function of pH (average of $n = 3$ independent experiments, error bars represent ± SD). The buffer solutions were acetate (pH 5.0), phosphate (pH 6.0, 7.0, and 8.0), and borate (pH 9.0 and 10.0) at concentrations of 100 mM, respectively. The other conditions were similar as in panel A. (C) Dependence of the photolysis quantum yield on the pH of the solution ($T = 22$ °C). The quantum yield was determined with the same procedure as discussed for pH 7.0 (see Materials and Methods), but the pH was varied from 5 to 10. The buffer solutions were the same as in panel B. Only data of the first three laser pulses were used for the analysis.

amino acids (*12*, *14*). This pH effect is relatively weak when compared to the expected 10-fold acceleration of k per pH unit for a purely proton-dependent process. The exact nature

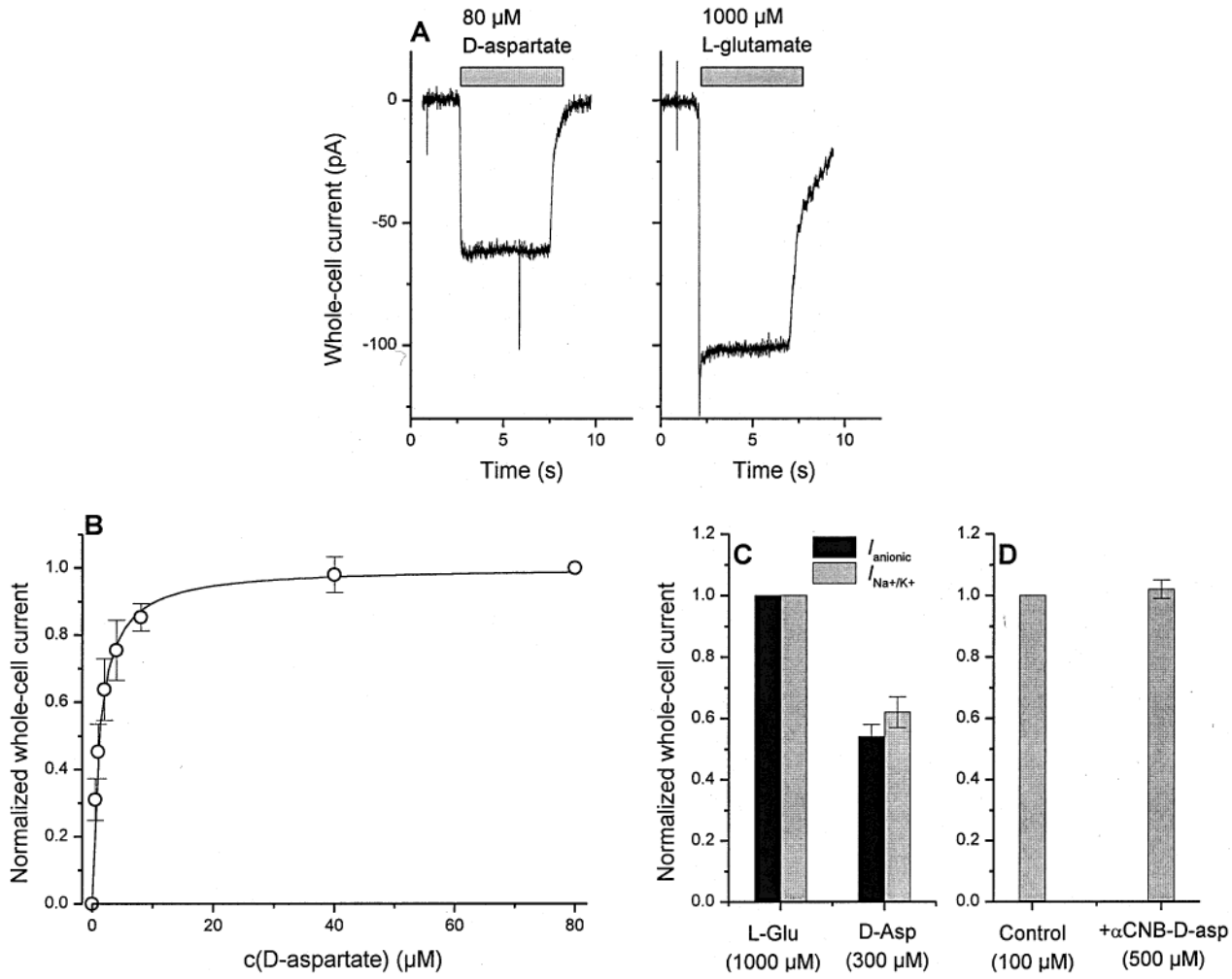

FIGURE 2: (A) Typical whole-cell current recordings of a EAAC1-expressing HEK293 cell upon rapid application of 80 μM D-aspartate (left panel) and 1000 μM L-glutamate (right panel), respectively (KSCN-based intracellular solution, $T = 22$ °C, pH 7.4, $V = 0$ mV). Application of the substrates with the rapid solution exchange device is indicated by the bars. Leak currents are subtracted. For $n = 5$ experiments with 2 cells, the ratio of the maximum currents at saturating substrate concentration between D-aspartate and L-glutamate was 0.54 ± 0.04. (B) Concentration dependence of the steady-state whole-cell current amplitude induced by rapid perfusion of D-aspartate in EAAC1-expressing HEK293 cells ($T = 22$ °C, pH = 7.3, transmembrane potential = 0 mV, $n = 6$; 4 cells). The data were normalized to the current response obtained at 80 μM D-aspartate. The intracellular solution contained 130 mM KSCN. The solid line represents the best fit to a Hill equation with the Hill coefficient $n = 1$ and an apparent dissociation constant of D-aspartate from the transporter of $K_m = 1.2 \pm 0.1$ μM. Error bars represent ± SD. (C) Relative steady-state whole-cell current amplitude induced by 1000 μM L-glutamate (left panel) and 300 μM D-aspartate (right panel). The black bars represent the coupled transport current (no electrochemical gradient for anions, KCl-based intracellular solution, $n = 6$, 3 cells), the gray bars the uncoupled anionic current (KSCN-based internal solution, $n = 6$, 3 cells). The transmembrane potential was 0 mV. (D) Relative whole-cell current amplitude induced by 100 μM D-aspartate in the absence (left, control) and presence of 500 μM caged D-aspartate (right). The data represent the average of three experiments with 2 different cells ($T = 22$ °C, pH = 7.3, $V = 0$ mV).

of the pH dependence of the *aci*-nitro intermediate decay is not known; however, one possible explanation would be that at the *aci*-nitro position protonated form of this species (7a, Scheme 1) is more reactive than its deprotonated form (7b, Scheme 1), a result that was confirmed by semiempirical calculations (*31*). In addition, we determined the pH dependence of the photolysis quantum yield. As shown in Figure 1, panel C, the quantum yield is maximal at pH 7 and drops off at both more acidic and more basic pH values. This effect is not caused by a pH dependence of the ground-state UV−visible spectrum, which is virtually unaffected by the pH (data not shown).

Steady-State EAAC1 Currents. The aim of this work was to apply α-CNB-caged D-aspartate to study the transport mechanism of EAAC1 on a molecular level. As a control, we first characterized the steady-state kinetic properties of EAAC1 upon D-aspartate activation. Rapid application of 80 μM D-aspartate evoked concentration-dependent EAAC1 whole-cell steady-state currents (Figure 2, panels A and B) in the presence of intracellular rhodanide. Under these conditions mainly the uncoupled anion component ($I_{anionic}^{Glu^-}$) of the current is observed. When L-glutamate was used instead of D-aspartate, we observed a small, rapidly decaying transient current component in addition to the steady-state current. The time resolution of the rapid solution exchange method, however, is insufficient to obtain detailed information about this current component (*21*).

The half-saturating concentration of the D-aspartate evoked steady-state current was 1.2 ± 0.1 μM, indicating that D-aspartate binds to the transporter with an about 4-fold higher apparent affinity than L-glutamate ($K_m = 5.1$ μM; ref *21*). However, the steady-state current induced by saturating

concentrations was reduced by a factor of 0.54 ± 0.04 (n = 5, 2 cells) with respect to L-glutamate as substrate in the presence of intracellular SCN^- (Figure 2, panel A). Therefore, this result suggests that D-aspartate is less potent in activating the steady-state anion conductance of EAAC1 than L-glutamate. When internal SCN^- is replaced by Cl^- the coupled transport current ($I^{Glu^-}_{Na^+/K^+}$) can be measured at V = 0 mV transmembrane potential (Figure 2, panel C). This current component ($I^{Glu^-}_{Na^+/K^+}$) is also reduced by a factor of 0.62 ± 0.05 (n = 10, 3 cells) when D-aspartate is applied to the transporter instead of L-glutamate, in the same range as published previously for the human EAAT3 expressed in *Xenopus* oocytes (0.82; ref *7*). This results indicates that the steady-state transport rate is smaller for D-aspartate than for L-glutamate.

Physiological Characterization of α*-CNB* D*-Aspartate*. First, we examined if the caged compound itself has an effect on the glutamate transporter. The results of these experiments are shown in Figure 2, panel D. D-Aspartate (100 μM) was applied to EAAC1 with a rapid solution exchange device in the absence and presence of 500 μM α-CNB-caged D-aspartate. The caged compound does not inhibit the transporter because the current amplitudes were identical in both experiments (n = 4, 2 cells), within experimental error. This result is consistent with previous studies on α-CNB-caged L-glutamate, which is also inactive with respect to EAAC1 in the same concentration range (*21*). Furthermore, α-CNB-caged D-aspartate in concentrations up to 100 μM caused no activation of EAAC1-mediated whole-cell currents. These results demonstrate that α-CNB-caged D-aspartate is biologically inert with respect to glutamate transporters.

Above α-CNB-caged D-aspartate concentrations of 100 μM, a small activation of EAAC1 currents was detected which is due to the small, but significant background of free D-aspartate in the sample presumably generated by spontaneous hydrolysis (less than 0.5%). This results in pre-flash activation of the transporter if excessive caged D-aspartate concentrations are used.

Pre-Steady-State EAAC1 Currents. Photorelease of D-aspartate from the caged precursor activates glutamate transporter-associated currents as shown in Figure 3 (right panel, middle trace). A solution of 400 μM caged D-aspartate was equilibrated for 500 ms with an EAAC1-expressing HEK293 cell before the compound was photolyzed by applying a 345-nm laser flash at time zero. Photolysis induced an inwardly directed whole-cell current that rises with a single-exponential time course to a maximum level, I_{ps}, within about 10 ms (time constant τ_{rise} = 1.8 ± 0.2 ms). This current rise is followed by a slower decay to a steady-state level, I_{ss}, of −19 pA. The time constant for this current decay is τ_{decay} = 45 ± 6 ms (n = 7, 3 cells) at 0 mV transmembrane potential. The time dependence of the current, $I(t)$, can be quantitatively described by the following equation (*21*):

$$I(t) = I_{ss} - I_{ps}\exp\left(-\frac{t}{\tau_{rise}}\right) + (I_{ps} - I_{ss})\exp\left(-\frac{t}{\tau_{decay}}\right) \quad (2)$$

The steady-state current amplitude evoked by rapid perfusion with 100 μM D-aspartate was −20 pA (Figure 3, left panel). We calculated a concentration of photoreleased D-aspartate of 40−50 μM from I_{ss} and the known dose response curve

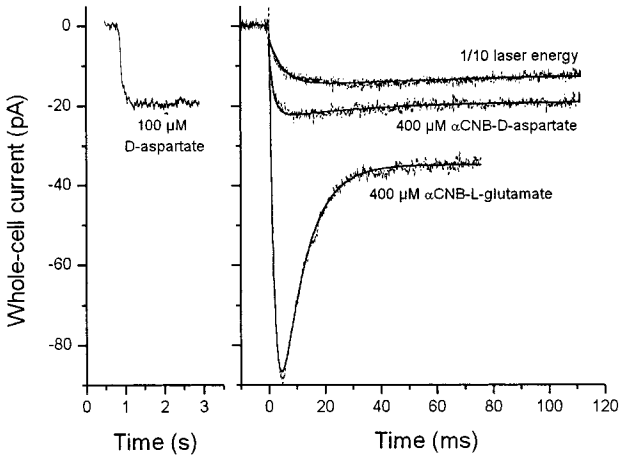

FIGURE 3: Laser-pulse photolysis experiment with α-CNB-caged D-aspartate (right panel, middle trace). Photolytic release of D-aspartate from the caged precursor (400 μM) activates a whole-cell current in EAAC1-expressing HEK293 cells. The laser energy was approximately 400 mJ/cm^2. The cell was pre-equilibrated with the caged compound for 500 ms before photolysis at time 0. The concentration of liberated D-aspartate was 40−50 μM as estimated by applying a standard concentration of 100 μM D-aspartate to the same cell with the rapid solution exchange device (left panel). A small background of free D-aspartate was present in the caged compound (<0.1%), leading to a slight preactivation of the transporter (about 5% of the total steady-state current, not shown). The solid line shows the best fit according to a biexponential function with time constants of 1.8 ± 0.1 ms (rising phase) and 50 ± 5 ms (decaying phase). In the upper trace, D-aspartate was released from 400 μM of its caged precursor under the same conditions, but the laser energy was attenuated by a factor of 10 using a neutral density filter. The concentration of liberated D-aspartate was estimated as 3 μM. The lower trace in the right panel shows a similar experiment, but L-glutamate was photolytically released from 400 μM of its α-CNB-caged precursor under the same conditions. The time constants obtained from the fit (solid line) were 1.7 ± 0.1 ms (rise) and 8.5 ± 0.2 ms (decay). The conditions of the experiment were T = 22 °C, pH = 7.3, V = 0 mV, KSCN-based intracellular solution.

(Figure 2, panel B). This is in the concentration range that was expected from previous experiments with α-CNB-caged L-glutamate under the same conditions (*21*) because of the similar photolysis quantum yield of both compounds. This result indicates that release of close to saturating concentrations of D-aspartate from the caged precursor can be achieved. Lowering the laser energy by a factor of 10 under identical conditions generated a smaller, subsaturating current, because only 3 μM D-aspartate were liberated (Figure 3, right panel, upper trace). Here, the whole-cell current rises more slowly with a time constant of 5 ± 1 ms, and no significant current decay is observed.

In contrast to D-aspartate, photolysis of α-CNB-L-glutamate under the same conditions as in the middle trace generated a more pronounced transient current component as demonstrated in Figure 3 (right panel, lower trace), consistent with previous results (*21*). The contribution of the transient component to the total current is 55 ± 2% (n = 7, 3 cells), whereas it is only 27 ± 7% (n = 6, 3 cells) when a D-aspartate concentration jump is applied (Figure 3). In addition, the rate of the current decay is about 6−7-fold faster for L-glutamate (τ = 8.5 ± 0.1 ms, Figure 3) than for D-aspartate. The steady-state and pre-steady-state kinetic properties of EAAC1 for D-aspartate and L-glutamate as substrates are summarized in Table 1. Together, the results

Table 1: Kinetic Properties of Substrate Transport by EAAC1 for D-Aspartate and L-Glutamate Determined under Steady-State and Pre-Steady-State Conditions[a]

	K_m (μM)	I_{max}/I_{max}(L-glu) transport current	I_{max}/I_{max}(L-glu) anion current	I_{ss}/I_{ps}	τ_{rise} (ms)	τ_{decay} (ms)
D-aspartate	1.2 ± 0.1	0.62 ± 0.05[c]	0.54 ± 0.04[c]	0.73 ± 0.07[d]	1.8 ± 0.2[d]	45 ± 6[d]
L-glutamate	5.1 ± 0.2[b]	1[c]	1[c]	0.45 ± 0.02[d]	1.3 ± 0.2[d]	7.9 ± 0.5[d]

[a] All values represent the average of at least 5 experiments with at least 2 different cells. [b] Ref *21*. [c] Rapid solution exchange, saturating substrate concentrations. [d] Laser-pulse photolysis, 400 μM caged substrate, approximately 40−50 μM photolytically released substrate.

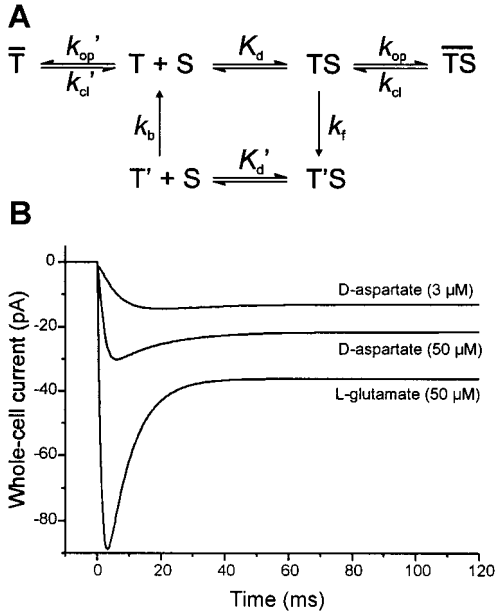

FIGURE 4: (A) Kinetic model for L-glutamate and D-aspartate transport by EAAC1 in the forward mode. Substrate (S) binding to the empty transporter, T, leads to the formation of the substrate-bound state, TS. After translocation the binding sites are exposed to the cytoplasm (state T′S) and substrate dissociation leads to population of state T′, which can undergo relocation to complete the transport cycle. Charge translocation is assumed to be quasi-irreversible (zero-trans conditions). Na^+, K^+, and proton binding steps were assumed to be in rapid preequilibrium and are, therefore, not included in the reaction scheme. The bar indicates anion-conducting states. (B) Numerical integration of the differential equations pertaining to the reaction mechanism shown in panel A. The conditions were chosen to match the experiments shown in Figure 3. The kinetic parameters were set to $k_f = 300\ s^{-1}$, $k_b = 40\ s^{-1}$, $K_d = 50\ \mu M$ (association rate constant = $2 \cdot 10^7\ M^{-1}\ s^{-1}$, dissociation rate constant = $1000\ s^{-1}$), $k_{op} = 1400\ s^{-1}$, and $k_{cl} = 700\ s^{-1}$ (L-glutamate). The activation of the anion-conducting state in the absence of glutamate (T̄) was neglected. For the simulation of the D-aspartate traces the parameters were identical, except $k_f = 30\ s^{-1}$, $k_{op} = 140\ s^{-1}$, and the dissociation rate constant was set to $100\ s^{-1}$ to account for the increased apparent D-aspartate affinity. For details of the simulation procedure see (*21*).

suggest a significant difference in the transport kinetics and properties of these two substrates.

Model for D*-Aspartate Transport by EAAC1.* Recently, we described the pre-steady-state kinetics of L-glutamate transport by EAAC1 with a basic model, incorporating substrate binding, translocation, and transporter relocation steps (*21*). This model is shown in Figure 4 and is also useful to interpret the experimental data that we obtained with D-aspartate. According to this model, the ratio of the steady-state and the pre-steady-state current, I_{ss}/I_{ps}, is a measure of the contribution to the rate limitation of the substrate translocation step versus the transporter relocation step. This ratio can be expressed as follows:

$$\frac{I_{ss}}{I_{ps}} = \frac{K_m^{ss}(S + K_m^{ps})}{K_m^{ps}(S + K_m^{ss})} \quad (3A)$$

$$= 1 - \frac{k_t}{k_b} \text{ for } S > K_m^{ps}, K_m^{ss} \quad (3B)$$

In this equation, S is the substrate concentration, K_m^{ps} and K_m^{ss} are the apparent substrate dissociation constants determined for the pre-steady-state and the steady-state current component, respectively (*21*), and k_t is the turnover rate constant of the transporter. k_b is the rate constant for the relocation of the empty carrier (see Figure 4). K_m^{ps} and K_m^{ss} can be expressed as

$$K_m^{ss} = \frac{K_d(1 + 1/\Phi_1)}{1 + 1/\Phi_2 + k_f/k_b} \quad (4A)$$

$$K_m^{ps} = \frac{K_d(1 + 1/\Phi_1)}{1 + 1/\Phi_2} \quad (4B)$$

Here, Φ_1 and Φ_2 are the equilibrium constants for formation of the anion-conducting states in the absence and presence of substrate, k_f represents the rate constant of substrate translocation, and K_d is the intrinsic substrate dissociation constant from the transporter (*21*). Using these equations, we estimated k_f for D-aspartate as approximately $30\ s^{-1}$ at 0 mV transmembrane potential, about a factor of 10 smaller than the respective value for L-glutamate (*21*). The value for k_b was set to $40\ s^{-1}$, estimated previously from the laser-pulse photolysis experiments with L-glutamate (*21*), showing that the change in the rate-limiting step of the transporter can quantitatively account for the reduced ratio I_{ss}/I_{ps} of 0.73 found for D-aspartate as compared to L-glutamate (0.46). Using these values for k_f and k_b, the turnover rate for D-aspartate was estimated as $k_t \sim 11\ s^{-1}$ (at 0 mV transmembrane potential and a D-aspartate concentration of 40−50 μM), about 2−3-fold smaller (eq 3) than the value found for L-glutamate (*21*). This explains the smaller maximum steady-state currents measured with D-aspartate as compared to L-glutamate as shown in Figure 2, panel C (*7*), and is in reasonable agreement with the ratio of the turnover rates for L-glutamate and D-aspartate of 1.6 calculated from the difference in the steady-state currents.

To further validate the basic kinetic model, we have performed numerical simulations (Figure 4, panel B) of EAAC1 currents generated by D-aspartate and L-glutamate concentration jumps using the conditions of the experiments shown in Figure 3. The values of the constants used for the simulation are based on those determined previously for L-glutamate (*21*). For the simulation of the D-aspartate traces, however, k_f and k_{op} were reduced 10-fold to 30 and $140\ s^{-1}$,

respectively. The simulated traces agree reasonably well with the experimental data, demonstrating the pronounced transient current component induced by L-glutamate activation of EAAC1 that is reduced and slowed upon D-aspartate activation. They also reproduce the delayed rise of the current and the absence of the current decay at subsaturating D-aspartate concentrations (upper trace, Figure 4, panel B) that was observed experimentally (Figure 3). This result demonstrates that D-aspartate binding may become rate-limiting for EAAC1 turnover at concentrations in the low micromolar range, as observed previously for L-glutamate as substrate (*21*).

DISCUSSION

Caged compounds have proven valuable tools for the investigation of transmembrane proteins because they enable one to determine relevant kinetic properties of these proteins with high time resolution. Recently, we have used laser-pulse photolysis of caged L-glutamate to study the glutamate transport process on a microsecond-to-millisecond time scale (*21*). Such studies are important because our understanding of the molecular mechanism of the glutamate transport process at present is limited; however, from the many different glutamate transporter substrates at present only L-glutamate is available in caged form. Here, we have extended the laser-pulse photolysis approach to the glutamate transporter substrate D-aspartic acid. D-Aspartic acid was protected as the β-ester with the α-carboxy-2-nitrobenzyl group. This photolabile protecting group has proven useful for the protection of a number of biologically important carboxylates in the past. Our results demonstrate that the α-CNB-precursor of D-aspartic acid does not differ in the biological activity from its counterpart α-CNB L-glutamic acid γ-ester. The compound neither activates nor inhibits the glutamate transporter subtype EAAC1. Furthermore, upon photolysis the liberated D-aspartate generates glutamate transporter-mediated whole-cell currents in EAAC1-transfected HEK293 cells.

In addition to the biological properties, we investigated the photochemical characteristics of the new caged D-aspartate. The compound has several desired properties such as a reasonable quantum yield of photolysis and a rapid rate constant of photodecomposition. These properties are very similar to the analogous L-glutamate derivative (γ-ester) (*11*) and derivatives of other carboxylic acids, such as GABA (*10*), kainic acid (*13*) and glycine (*14*), demonstrating once again the usefulness of the α-CNB-group for protecting these biologically important compounds. We put special emphasis on the pH dependence of the caged D-aspartate photolysis process because glutamate transport is highly pH dependent, and the compound may, therefore, be used for kinetic studies at a pH very different from the physiological range. The photolysis of caged D-aspartate is slowed to some extent at low proton concentrations. However, even at pH 10, the photolysis rate constant of 17000 s^{-1} is about four times faster than the rate constants of the fastest glutamate transporter reactions that have been observed at present. The photolysis quantum yield decreases at both low and high proton concentrations. Nevertheless, it will be sufficient over the pH range between 5 and 10 to photolytically release D-aspartate concentrations high enough for kinetic studies of the glutamate transporter.

As found for other nitrobenzyl-caged compounds, the decay of the *aci*-nitro intermediate of α-CNB-caged D-aspartic acid is biphasic. Possible explanations for the two components would be that they represent the reaction of two different isomeric forms (E-, Z-isomers) (*31*) or protonated and deprotonated forms of the *aci*-nitro intermediate (*32*). In the first case, both phases of the transient absorption change should be pH dependent, which is not found experimentally. In the second case, protonation or deprotonation of the nitronate anion should be considerably faster than the rates for the *aci*-nitro decay observed here (*32*). Therefore, both explanations are not satisfactory, and the clarification of the photolysis mechanism must await further, more detailed experiments.

What is the significance of these rapid kinetic experiments for our understanding of the function of glutamate transporters? The rate of glutamate transport by the high affinity glutamate transporters is highly dependent on the transported substrate (*7*, *33*). In general, D-aspartate is transported at a lower rate than L-glutamate (*7*). Therefore, the comparative analysis of rapid transporter kinetics for both of these substrates provides valuable information about the rate limitation of specific transporter reaction steps. We have suggested previously that translocation of L-glutamate is not rate limiting for the turnover of the glutamate transporter subtype EAAC1 (*21*). This hypothesis can now be tested with pre-steady-state kinetic measurements using D-aspartate as a substrate instead of L-glutamate. The pronounced pre-steady-state transient current component induced by L-glutamate concentration jumps is only observed to a minor extent with D-aspartate (Figure 3), indicating that the D-aspartate translocation becomes the rate-limiting step in the EAAC1 transport cycle. Instead, for L-glutamate as substrate, we proposed that the K^+-driven relocation of the transporter is rate-limiting (*21*), in contrast to previous suggestions (*5*).

D-Aspartate is less efficiently transported by EAAC1 than L-glutamate. Is it also less efficient in activating the anion conductance? Our data indicate that this is the case because (i) the steady-state current carried by anions at saturating D-aspartate concentrations is only 60% of that induced by L-glutamate, and (ii) this current rises more slowly when a D-aspartate concentration jump is applied as compared to a L-glutamate concentration jump of the same concentration (Table 1). These results suggest that in EAAC1 formation of the anion-conducting state and glutamate translocation are kinetically tightly coupled. If the formation kinetics of the anion-conducting state was not affected by different types of substrate one would expect that the D-aspartate-induced anion current would be larger than that elicited by L-glutamate because of the differences in translocation rates. In fact, such a behavior is observed for another glutamate transporter subtype, GLAST (*34*). Here, D-aspartate induces a larger anionic current than L-glutamate. This might reflect differences in the functional properties of these two transporter subtypes.

With the availability of the new caged D-aspartic acid derivative with its desirable photochemical and biological properties, it will now be possible to obtain further information about the molecular mechanism of the high affinity glutamate transport process by applying rapid chemical kinetic techniques. This information is difficult to obtain with

rapid solution exchange techniques because of inadequate time resolution when used together with whole-cell current recording. In general, sufficient time resolution can be achieved by rapid perfusion of excised membrane patches with supersaturating concentrations of substrate (*35*), however, the smaller membrane area of patches may present a problem. Glutamate transporter currents are typically small with conductances in the range of fS to low pS (*21*, *34*, *36*). Thus, even with high density expression of transporters, the currents are near the detection limit in membrane patches. Whole cells typically provide at least a 100-times larger surface area than excised patches, and thus their use circumvents these problems. Therefore, laser-pulse photolysis of caged glutamate transporter substrates together with current recording from whole cells is the most promising method for the investigation of rapid transporter kinetics.

In addition to kinetic experiments, the new compound can be used for locating glutamate transporters in functional neuronal circuits. For this purpose it is advantageous with respect to caged L-glutamate because D-aspartate binds selectively to the glutamate transporters with high affinity. Not much is known about the agonistic properties of D-aspartate with respect to glutamate receptor activation. However, it is believed that D-aspartate activates only the *N*-methyl-D-aspartate (NMDA) subtype of the glutamate receptor family with an affinity of about 50 μM (*37*). This value is about 40-fold higher than the apparent affinity of D-aspartate for EAAC1 determined here. It can be, therefore, expected that caged D-aspartate can be used to selectively activate glutamate transporters in neuronal cell cultures or brain slices.

ACKNOWLEDGMENT

We thank E. Bamberg for critical reading of the manuscript and E. Bamberg, H.-D. Martin and H. Wässle for continuous encouragement and support.

REFERENCES

1. Kandel, E. R., Schwartz, J. H., and Jessell, T. M. (1995) *Essentials of Neural Science and Behavior*, Appleton & Lange.
2. Clements, J. D. (1996) *Trends Neurosci. 195*, 163−171.
3. Diamond, J. S., and Jahr, C. E. (1997) *J. Neurosci. 17*, 4672−87.
4. Kanner, B. I., and Sharon, I. (1978) *Biochemistry 17*, 3949−3953.
5. Kanai, Y., Nussberger, S., Romero, M. F., Boron, W. F., Hebert, S. C., and Hediger, M. A. (1995) *J. Biol. Chem. 270*, 16561−16568.
6. Pines, G., Danbolt, N. C., Bjoras, M., Zhang, Y., Bendahan, A., Eide, L., Koepsell, H., Storm Mathisen, J., Seeberg, E., and Kanner, B. I. (1992) *Nature 360*, 464−467.
7. Arriza, J. L., Fairman, W. A., Wadiche, J. I., Murdoch, G. H., Kavanaugh, M. P., and Amara, S. G. (1994) *J. Neurosci. 14*, 5559−5569.
8. Adams, S. R., and Tsien, R. Y. (1993) *Annu. Rev. Physiol. 55*, 755−784.
9. Milburn, T., Matsubara, N., Billington, A. P., Udgaonkar, J. B., Walker, J. W., Carpenter, B. K., Webb, W. W., Marque, J., Denk, W., and et al. (1989) *Biochemistry 28*, 49−56.
10. Wieboldt, R., Ramesh, D., Carpenter, B. K., and Hess, G. P. (1994) *Biochemistry 33*, 1526−33.
11. Wieboldt, R., Gee, K. R., Niu, L., Ramesh, D., Carpenter, B. K., and Hess, G. P. (1994) *Proc. Natl. Acad. Sci. U.S.A. 91*, 8752−8756.
12. Gee, K. R., Niu, L., Schaper, K., and Hess, G. P. (1995) *J. Org. Chem. 60*, 4260−4263.
13. Niu, L., Gee, K. R., Schaper, K., and Hess, G. P. (1996) *Biochemistry 35*, 2030−6.
14. Grewer, C., Jäger, J., Carpenter, B. K., and Hess, G. P. (2000) *Biochemistry 39*, 2063−2070.
15. Denk, W. (1994) *Proc. Natl. Acad. Sci. U.S.A. 91*, 6629−6633.
16. Callaway, E. M., and Katz, L. C. (1993) *Proc. Natl. Acad. Sci. U.S.A. 90*, 7661−7665.
17. Li, H., Avery, L., Denk, W., and Hess, G. P. (1997) *Proc. Natl. Acad. Sci. U.S.A. 94*, 5912−5916.
18. Takimoto, S., Inanaga, J., Katsuki, T., and Yamaguchi, M. (1976) *Bull. Chem. Soc. Jpn.* 2335−2336.
19. Chen, C., and Okayama, H. (1987) *Mol. Cell. Biol. 7*, 2745−52.
20. Hamill, O. P., Marty, A., Neher, E., Sakmann, B., and Sigworth, F. J. (1981) *Pflugers Arch. Eur. J. Physiol. 391*, 85−100.
21. Grewer, C., Watzke, N., Wiessner, M., and Rauen, T. (2000) *Proc. Natl. Acad. Sci. U.S.A. 97*, 9706−9711.
22. Grewer, C. (1999) *Biophys. J. 77*, 727−738.
23. Krishtal, O. A., and Pidoplichko, V. I. (1980) *Neuroscience 5*, 2325−7.
24. Rossi, F. M., Margulis, M., Tang, C. M., and Kao, J. P. Y. (1997) *J. Biol. Chem. 272*, 32933−32939.
25. McCray, J. A., Herbette, L., Kihara, T., and Trentham, D. R. (1980) *Proc. Natl. Acad. Sci. U.S.A. 77*, 7237−7241.
26. Schupp, H., Wong, W. K., and Schnabel, W. (1987) *J. Photochem. 36*, 85−97.
27. Walker, J. W., Reid, G. P., McCray, J. A., and Trentham, D. R. (1988) *J. Am. Chem. Soc. 110*, 7170−7177.
28. Wootton, J. F., and Trentham, D. R. (1989) *NATO Adv. Study Inst. Ser. C 272*, 277−296.
29. Nelson, P. J., Dean, G. E., Aronson, P. S., and Rudnick, G. (1983) *Biochemistry 22*, 5459−5463.
30. Zerangue, N., and Kavanaugh, M. P. (1996) *Nature 383*, 634−637.
31. Schaper, K., Dommaschke, D., Globisch, S., and Madani-Mobarekeh, S. A. (2000) *J. Inf. Rec. 25*, 339−354.
32. Ellis-Davies, G. C. R., Kaplan, J. H., and Barsotti, R. J. (1996) *Biophys. J. 70*, 1006−1016.
33. Kanai, Y., Stelzner, M., Nussberger, S., Khawaja, S., Hebert, S. C., Smith, C. P., and Hediger, M. A. (1994) *J. Biol. Chem. 269*, 20599−20606.
34. Wadiche, J. I., and Kavanaugh, M. P. (1998) *J. Neurosci. 18*, 7650−7661.
35. Liu, Y., and Dilger, J. P. (1991) *Biophys. J. 59*.
36. Picaud, S. A., Larsson, H. P., Grant, G. B., Lecar, H., and Werblin, F. S. (1995) *J. Neurophysiol. 74*, 1760−1771.
37. Kubrusly, R. C. C., de Mello, M. C. F., and de Mello, F. G. (1998) *Neurochem. Int. 32*, 47−52.

BI0015919